Construction and Building Materials 111 (2016) 317–325

Contents lists available at ScienceDirect

Construction and Building Materials

journal homepage: www.elsevier.com/locate/conbuildmat

Synthesis and strength optimization of one-part geopolymer based on red mud

Nan Ye [a], Jiakuan Yang [a,*], Sha Liang [a], Yong Hu [a], Jingping Hu [a], Bo Xiao [a], Qifei Huang [b]

[a] School of Environmental Science and Engineering, Huazhong University of Science and Technology (HUST), 1037 Luoyu Road, Wuhan, Hubei 430074, PR China
[b] State Key Laboratory of Environmental Criteria and Risk Assessment, Chinese Research Academy of Environmental Sciences, Beijing 100012, PR China

HIGHLIGHTS

- One-part geopolymer was synthesized by using Bayer red mud as main raw material.
- Long-term strength of binder was significantly improved with addition of 20–30 wt% SF.
- Lower water/solid ratio contributed to increasing the strength.
- The compressive strength of geopolymer cured for 28 d reached 31.5 MPa.
- Geopolymerization of dissolved aluminosilicate and silica formed dense matrices.

GRAPHICAL ABSTRACT

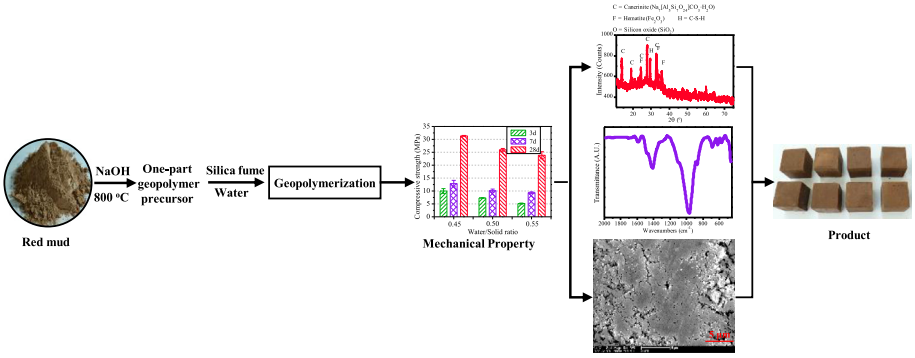

ARTICLE INFO

Article history:
Received 13 June 2015
Received in revised form 23 January 2016
Accepted 19 February 2016
Available online 23 February 2016

Keywords:
Bayer red mud
One-part geopolymer
Alkali–thermal activation
Sodium aluminosilicate
Silica fume

ABSTRACT

One-part geopolymer was synthesized from alkali–thermal activated Bayer red mud (RM) with addition of silica to optimize its composition. The RM was pretreated through alkali–thermal activation and turned to geopolymer precursor, which could be used by only adding water in blending process. However the long-term strength of the binder with only RM was poor because of the unstable polymerization due to the low SiO_2/Al_2O_3 molar ratio (1.41). Silica fume (SF) was chosen to increase the SiO_2/Al_2O_3 molar ratio of the geopolymer formulation. By adding 25 wt% of SF, the 28 d compressive strength of the geopolymer with a SiO_2/Al_2O_3 molar ratio of 3.45 could reach 31.5 MPa at a water/solid ratio of 0.45. Sodium aluminosilicate in the activated RM dissolved in water and formed an alkaline environment to dissolve SF. The dissolved silica participated in geopolymerization, leading to a satisfactory geopolymer composition. Typical amorphous geopolymer matrices were formed in the binder completely cured.

1. Introduction

Bayer red mud (RM) or bauxite residue is the residue of bauxite ores after digestion by caustic soda through the Bayer process to produce alumina. It is a high alkaline waste with an average pH of 11.3 ± 1.0 [1] and is classified as a toxic industrial waste [2]. The high alkalinity and superfine particle size make proper disposal of RM difficult. Most of RM is still disposed through storage on land, including lagooning, dry stacking, and dry cake disposal [3]. But land disposal may cause serious environmental pollution, if RM was leaked into the surrounding environment. Ecological disasters caused by RM dam-break have occurred for many times, such as the event in Hungary in 2010 [4].

The research of economical alternatives to utilize red mud have been carried out for more than 50 years. Numerous application

* Corresponding author.
E-mail address: jkyang@mail.hust.edu.cn (J. Yang).

http://dx.doi.org/10.1016/j.conbuildmat.2016.02.099
0950-0618/

possibilities have been researched and developed. The main research areas could be summarized as: metallurgical applications [5], filler or substrate for composite materials [6], catalysts [7], adsorbents [8], construction and building materials [9]. Despite thousands of publications and patents on the subject have been published, large-scale utilization of RM is still absent. Klauber et al. summarized the barriers that need to be overcome for RM utilization as: volume, performance, cost and risk [10]. Research to refine the utilization technology still needs to be conducted. Among the utilization options, construction and building materials pose lower risk for implementation. Manufacture of geopolymers based on RM including controlled low strength materials are one of the suggested research project [10].

Geopolymer poses as a viable alternative for utilizing RM in building materials to avoid the alkali-aggregate reaction since alkali is a necessary component for geopolymer. In recent decades, geopolymer has been attracting worldwide attentions for their low CO_2 emissions and high properties. Geopolymers are synthesized by activating solid aluminosilicate sources with alkali metal hydroxide or silicate solutions through a series of dissolution–reorientation–solidification reactions [11]. The binding property of the geopolymer results from the amorphous alkali aluminosilicate gels, which have a general formula as $M_n[-(Si-O_2)_z-Al-O]_n \cdot wH_2O$, wherein M represents one or more alkali metals and z is 1, 2 or 3 [12]. Some geopolymers also contain alkaline earth cations, particularly Ca^{2+} based on industrial wastes such as granulated blast furnace slag or fly ash, but it's not sure whether the alkaline earth cations are actually incorporated into the geopolymer structure [13]. The satisfactory geopolymer compositions are suggested to be in the range of M_2O/SiO_2, 0.2–0.48; SiO_2/Al_2O_3, 3.3–4.5; and H_2O/M_2O, 10–25 [14].

RM is not a quite ideal material for preparing geopolymer directly due to its poor activity and low SiO_2/Al_2O_3 molar ratio (lower than 2), thus it is usually pretreated and mixed with other materials to prepare geopolymer. Some researches have been done by combining RM with other excellent geopolymer precursors such as metakaolin [15], fly ash [16–18], and rice husk ash [19] and using sodium hydroxide or sodium silicate solutions as an activator to synthesize geopolymer. In our previous study [20], a type of geopolymer was synthesized from thermal-pretreated RM and granulated blast furnace slag by using sodium silicate as the activator. These geopolymers synthesized by mixing solid aluminosilicate sources with an alkaline activator solution were called as two-part geopolymer for their two-part mix process, which was the conventional design of geopolymer. If the alkali came from the solid phase, and the blending process was just one-part mix (i.e. only need to add water), geopolymer would present the convenience of ordinary Portland cement (OPC). Koloušek et al. proposed the new procedure for synthesizing geopolymer based on direct calcinations of low-quality kaolin with Na/K hydroxides to get one-part geopolymer precursor [21]. Feng et al. synthesized a one-part geopolymer from albite by calcinating it with addition of NaOH and Na_2CO_3 [22]. One-part geopolymers would present opportunities beyond the traditional two-part geopolymers because one-part geopolymers were ideal for large-scale deployment, as most of the quality control can be dealt with centrally [23].

In the previous work, a one-part geopolymer had been synthesized from Bayer red mud through an alkali–thermal activation process [24]. But the binder collapsed in long-term curing after 7 d since the polymerization of Al–O and Si–O was unstable due to its low SiO_2/Al_2O_3 molar ratio of only 1.41 [24], much lower than the appropriate range of 3.3–4.5. This article presents a research on solving the strength deterioration problem of the one-part geopolymer synthesized from Bayer red mud, by adding another silica-rich material with high activity – silica fume (SF) – to improve the SiO_2/Al_2O_3 molar ratio of the binder, thus to improve the stability of the product.

2. Material and methods

2.1. Raw materials

A local Bayer red mud, provided by an alumina plant of Chalco Co. in Zhengzhou, China, was dried to constant weight at 105 °C and grinded to pass a 0.30 mm mesh sieve. It was a typical residue from the Bayer process to produce alumina using Chinese low-Fe diaspore bauxite ores [25]. The particle size of the RM was in the range of 0.1–70 μm with a median diameter (d_{50}) of 3.5 μm as determined by laser granulometry. A condensed silica fume, provided by China Construction Ready Mixed Concrete Co. Ltd. in Wuhan, China, was used to improve the SiO_2/Al_2O_3 molar ratio of the formulations. SF is a by-product of the manufacture of silicon or of various silicon alloys. The particle size of the SF was in the range of 0.25–150 μm with a d_{50} of 23.66 μm as determined by laser granulometry. The chemical compositions of the raw materials are presented in Table 1, which were detected by an Axios Advanced X-ray Fluorescence Spectrometer (XRF). The RM is an alkaline aluminosilicate source with a SiO_2/Al_2O_3 molar ratio of 1.41 and the SF is a silica-rich source with 94.43 wt% of SiO_2.

The mineral phases of raw RM and SF were investigated by the powder X-ray diffractometry (XRD), using an Empyrean (PANalytical B.V., Holland) with Cu Kα radiation and $\lambda = 1.5418$ Å, operated at 40 mA, 40 kV with a scanning rate of 0.2785°/s for 2θ in the range from 10° to 75°. The XRD patterns of the mineral phases of RM and SF are shown in Fig. 1. The mineral phases in the raw RM include gibbsite, hematite, calcite, cancrinite, muscovite-2, and katoite. Cancrinite is a group of normal zeolitic mineral in alkaline massifs as a rock-forming mineral, and has the common generalized formula $(Na, Ca, K)_{7-8}[(Si, Al)_{12}O_{24}](CO_3, OH)_2 \cdot 2-3H_2O$ [26]. The aluminosilicates were mainly in the crystal form with low activity, such as cancrinite, muscovite-2, and katoite. The SF mainly consist of amorphous active silica, with a little of unburnt carbon in the form of silicon carbide.

2.2. Alkali–thermal activation of red mud

To get one-part geopolymer precursors from Bayer RM, the RM was pretreated through an alkali–thermal activation process. RM samples were mixed with sodium hydroxide pellets of analytical grade (99.9%), and calcined at 800 °C for 1 h in a muffle furnace, and then cooled naturally in the furnace to room temperature. Two specified amounts of sodium hydroxide were chosen, 10 and 15 wt% (based on Na_2O with respect to the mass of RM), and the corresponding alkali–thermal activated RM were called RM-10N and RM-15N, respectively. The alkali–thermal activated RM was grinded in a sample preparation comminuter for 3 min to pass a 0.3 mm mesh sieve.

2.3. Synthesis of one-part geopolymer

To design one-part geopolymer with different formulations, the alkali–thermal activated RM were mixed with 0, 5, 10, 15, 20, 25, 30 wt% of SF with respect to the mass of total solid to produce different geopolymer precursors. The geopolymer precursors were then mechanically blended with water at a water/solid ratio of 0.65 for 5 min to obtain homogeneous pastes. The binder made from RM has strong absorbing capacity of water due to the superfine particle-size distribution and large surface area of RM. To get a geopolymer with higher strength, the water/solid ratio was decreased. The water/solid ratios of 0.60 and 0.55 were adopted for formulations at the SF addition of 25 wt%. It was known that sodium lignosulphonate was usually used as dispersant to improve the flowability and workability of concrete [27]. By adding 0.5 wt% of sodium lignosulphonate as dispersant, the water/solid ratios were further reduced from 0.55 to 0.45.

The pastes were then moulded in steel molds (40 × 40 × 40 mm) and covered by plastic films and then cured at 20 ± 1 °C for 24 h. The binders were then demoulded and sealed in polyethylene zip-lock bags and cured again under the same condition. Afterwards, the compressive strengths of the binders cured for 3, 7 and 28 d were measured using a YAW-300 automatic compression testing machine (Kent mechanical & electrical Co., China). Each set of binders had triplicates. The formulation designs of one-part geopolymers are shown in Table 2, and the experimental designs of the effect of water/solid ratio on the compressive strength are presented in Table 3.

In addition, control tests without alkali–thermal activation were also carried out. The same dosages of NaOH pellet were added after the RM sample was directly calcined at 800 °C, and then mixed with 0, 10, 20 wt% of SF. But the binders prepared from the mixtures at a water/solid ratio of 0.65 were not able to harden, and showed no enough strength for demould.

2.4. Leaching test

Leaching tests for the one-part geopolymer binders prepared from RM-10N with different SF addition and water/solid ratio were performed to study the transformation of pH. The binders were crushed into particles with a size lower than 2.38 mm, and then leached in deionized water at a liquid/solid (L/S) ratio of 20:1 for 18 h. The pHs of the leaching solutions were then measured.

Table 1
Chemical compositions of RM and SF.

Components (wt%)	SiO_2	Al_2O_3	Fe_2O_3	Na_2O	CaO	TiO_2	K_2O	MgO	SO_3	LOI*
RM	20.38	24.50	9.48	11.46	12.86	2.92	0.88	1.00	0.67	15.40
SF	94.43	0.27	0.14	0.25	0.28	–	0.30	0.29	0.24	3.61

LOI*: loss on ignition, mass loss at 1200 °C.

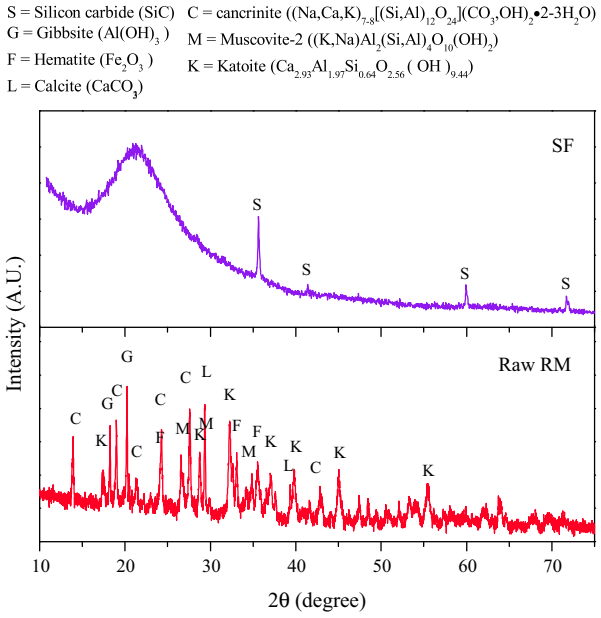

Fig. 1. The XRD patterns of raw RM sample and SF.

2.5. Material characterization

The mineral phases of alkali–thermal activated RM and geopolymer binders were investigated by the powder XRD at the same experimental conditions described in Section 2.1. Fourier-transform infrared spectroscopy (FTIR) tests were performed by Vertex 70 (Bruker Co., Germany) with a wavelength of 450–4000 cm^{-1}. The morphological and elemental analysis of the typical binders with fractured surfaces was conducted by field emission scanning electron microscope (FE-SEM) after coating with Au for 300 s, using Sirion 200 (FEI Co., Holland), at a operating voltage of 10.00 kV.

3. Results and discussion

3.1. The pH transformation of the binders

The pHs of leaching solutions of the one-part geopolymer binders prepared from RM-10N are shown in Fig. 2. The leaching solution of the one-part geopolymer binders pose alkaline, with pHs varying in the range of 11.2–13.2. The alkaline environment in the geopolymer binders results from the dissolution of sodium aluminosilicates in alkali–thermal activated RM, and the pH declines with the increase of SF addition. When the curing age is extended from 3 d to 7 d, the pHs decline, and the reduction ratio increase with SF addition. The same transformation is observed in the binders with 15–30 wt% of SF at the curing age of 28 d. The dissolution of SF in alkaline environment will consume OH^- ions in the liquid phase of the binders and cause the pH decline. But for the binders with 0–10 wt% of SF, the 28 d pHs are even higher than that of 3 d and 7 d. This should be a consequence of the depolymerization or re-dissolution of the aluminosilicate gels with low SiO_2/Al_2O_3 molar ratio.

As shown in Fig. 2, the water/solid ratio has little influence on the pH of the geopolymer binder. But the 3 d and 7 d pHs of the binders with 0.5 wt% of sodium lignosulphonate are higher than that of the binders with no addition of sodium lignosulphonate. The dissolution of SF and polymerization of aluminosilicate seems to be retarded at the early stage at the influence of sodium lignosulphonate. The 28 d pHs of them show no visible differences, implying that the dissolution of SF and polymerization of aluminosilicate get back to normal at the curing age of 28 d.

3.2. The effect of SF addition on the compressive strength

The effects of SF addition on the compressive strength of the one-part geopolymer binders are shown in Fig. 3. The one-part geopolymer binders produced from RM-10N and RM-15N hardened quickly and developed strength after 24 h. The alkali–thermal

Table 2
Formulation designs of one-part geopolymer.

No.	Alkali–thermal RM		SF addition/wt%	Water/solid ratio	Molar ratio in binders		
	Class	Addition/wt%			Na_2O/SiO_2	SiO_2/Al_2O_3	H_2O/Na_2O
G-10N	RM-10N*	100	0	0.65	1.02	1.41	9.72
G-10N-5S		95	5		0.83	1.74	10.23
G-10N-10S		90	10		0.69	2.09	10.80
G-10N-15S		85	15		0.58	2.49	11.44
G-10N-20S		80	20		0.49	2.94	12.15
G-10N-25S		75	25		0.42	3.45	12.96
G-10N-30S		70	30		0.36	4.03	13.89
G-15N	RM-15N*	100	0	0.65	1.26	1.41	8.32
G-15N-5S		95	5		1.01	1.75	8.76
G-15N-10S		90	10		0.83	2.13	9.25
G-15N-15S		85	15		0.70	2.55	9.79
G-15N-20S		80	20		0.59	3.03	10.41
G-15N-25S		75	25		0.50	3.56	11.10
G-15N-30S		70	30		0.43	4.18	11.89

* RM-10N and RM-15N represent the alkali–thermal activated RM calcined at 800 °C for 1 h with 10 and 15 wt% amounts of Na_2O in sodium hydroxide (referred to mass ratio of Na_2O to RM), respectively.

Table 3
Experimental designs of the effect of water/solid ratio on the compressive strength.

No.	Alkali–thermal red mud	Silica fume addition/wt%	Water/solid ratio	Sodium lignosulphonate addition /wt%
G-10N-25S-A1	RM-10N	25	0.65	0
G-10N-25S -A2			0.60	
G-10N-25S -A3			0.55	
G-15N-25S -A1	RM-15N	25	0.65	0
G-15N-25S -A2			0.60	
G-15N-25S -A3			0.55	
G-10N-25S -B1	RM-10N	25	0.55	0.5
G-10N-25S -B2			0.50	
G-10N-25S -B3			0.45	

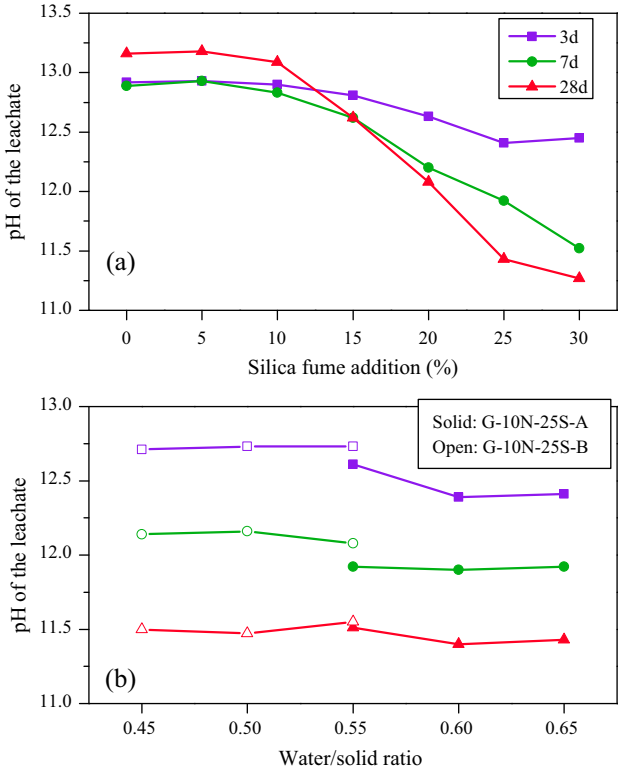

Fig. 2. The pHs of leaching solutions of the one-part geopolymer binders prepared from RM-10N.

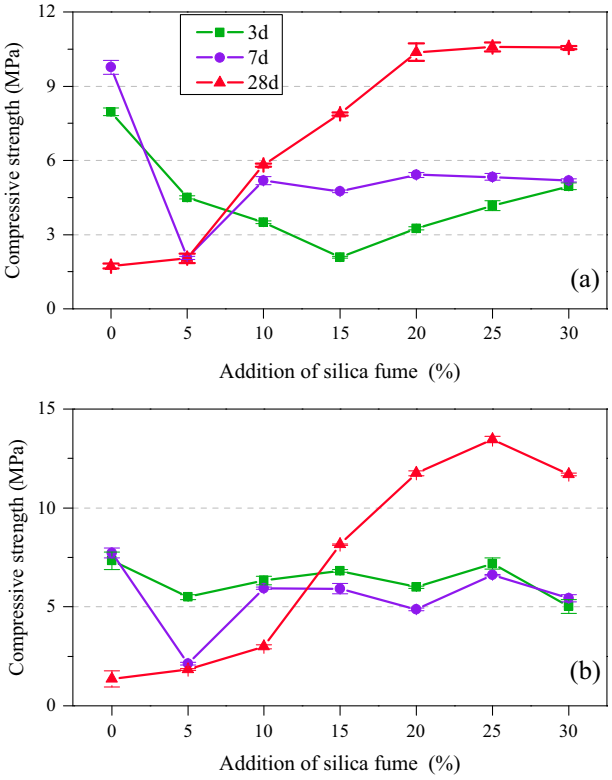

Fig. 3. The effect of SF addition on the compressive strength of one-part geopolymer binders prepared from alkali–thermal activated RM: (a) RM-10N; (b) RM-15N.

activation process seems to be quite effective for producing one-part geopolymer by comparison with the results of control tests without alkali–thermal activation, which showed no enough strength for demould. But both the compressive strengths of the G-10N and G-15N binders with no SF decrease significantly when the curing age is extended from 7 d to 28 d. The binders with 5 wt% of SF show the similar deterioration phenomenon since the curing age of 7 d. The strength decline with further curing may be a consequence of the depolymerization or dissolution of the aluminosilicate resulting from the low SiO_2/Al_2O_3 molar ratio of the formulations, which have been demonstrated by the increased pHs at 28 d of the binders with 0–10 wt% of SF in Fig. 2. Associated processes such as carbonation, and efflorescence would also cause degradation of the matrices and undermine the strength of geopolymer [24,28].

The compressive strengths of binders cured for 3 d and 7 d change a little with the increase of SF from 5 wt% to 30 wt% for both geopolymer binders. However, the 28 d compressive strength increases dramatically with the increase of SF addition from 5 wt% to 25 wt%. As shown in Table 2, the designed formulations of the one-part geopolymer approach the satisfactory compositions in the range of M_2O/SiO_2, 0.2–0.48; SiO_2/Al_2O_3, 3.3–4.5; H_2O/M_2O, 10–25 [14], at the SF addition of 20–30 wt%, especially at 25 wt%. It is consistent with the compressive strength results shown in Fig. 3. The addition of SF has more significant effects on the long-term strength of binders than the early strength. This is mainly because that the dissolution of SF is relatively slow, thus SF plays its role mainly in the long-term curing. Dissolved silica from SF particles can improve the SiO_2/Al_2O_3 molar ratio of the gels in the binders. Moreover, the dissolved silicates and aluminates in the gels polymerize to form aluminosilicate gels with better formulations in the long-term curing, leading to a higher compressive strength at the curing age of 28 d. Generally, the compressive strength of the binder made from RM-15N is relatively higher than that from RM-10N, mostly because that G-15N group has higher Na_2O/SiO_2 ratio, which will contribute to the dissolution of SF.

3.3. The effect of water/solid ratio on the compressive strength

The effects of water/solid ratio on the strength of one-part geopolymer are shown in Fig. 4. The compressive strengths of the binders cured for 3 d and 7 d increase a little when the water/solid ratio decreases from 0.65 to 0.55 for both G-10N-25S and G-15N-25S. However, the 28 d compressive strengths increase significantly, especially for G-10N-25S. At the water/solid ratio of 0.65, the compressive strengths of G-10N-25S are significantly lower than that of G-15N-25S. But at the water/solid ratio of 0.55, the compressive strength of G-10N-25S-A3 is close to that of G-15N-25S-A3, probably because that the role of pH is unconspicuous at lower water/solid ratio. Therefore, RM-10N poses to be better than RM-15N for synthesizing one-part geopolymer for less sodium hydroxide demand.

In Fig. 4(c), the water/solid ratio of G-10N-25S binder was reduced to 0.45 by adding 0.5 wt% of sodium lignosulphonate as dispersant. A further increase of the compressive strength is obtained, which reaches 31.5 MPa at the water/solid ratio of 0.45 at the curing age of 28 d. It is well known that an decrease in the water/solid ratio would decrease the porosity and increase the compactness of the material as well as the mechanical strength [29]. Sodium lignosulphonate acts as setting retardant in the one-part geopolymer binder. The 3 d compressive strength of G-10N-25S-B1 with 0.5 wt% sodium lignosulphonate is lower than that of G-10N-25S-A3 with the same water/solid ratio. It has been shown in Fig. 2 that the pHs of G-10N-25S-B1 cured for 3 d and 7d are higher than that of G-10N-25S-A3, implying that the dissolution of SF and polymerization of aluminosilicates is retarded at the early stage. But the compressive strength of G-10N-25S-B1 cured for 28 d are higher than G-10N-25S-A3 for about 4 MPa. Geopolymer gels with more desirable formations should have been formed through the delayed polymerization of aluminosilicates.

With an optimum addition (25 wt%) of SF and a satisfactory water/solid ratio (0.45), the one-part geopolymer could obtain appropriate strength for some practical use. It could potentially replace ordinary clay bricks for inner-wall or backing bricks and other non-load bearing construction materials. This one-part geopolymer material presents intrinsic red color due to the content of iron compounds from RM, and the potential coating process for some use could be omitted.

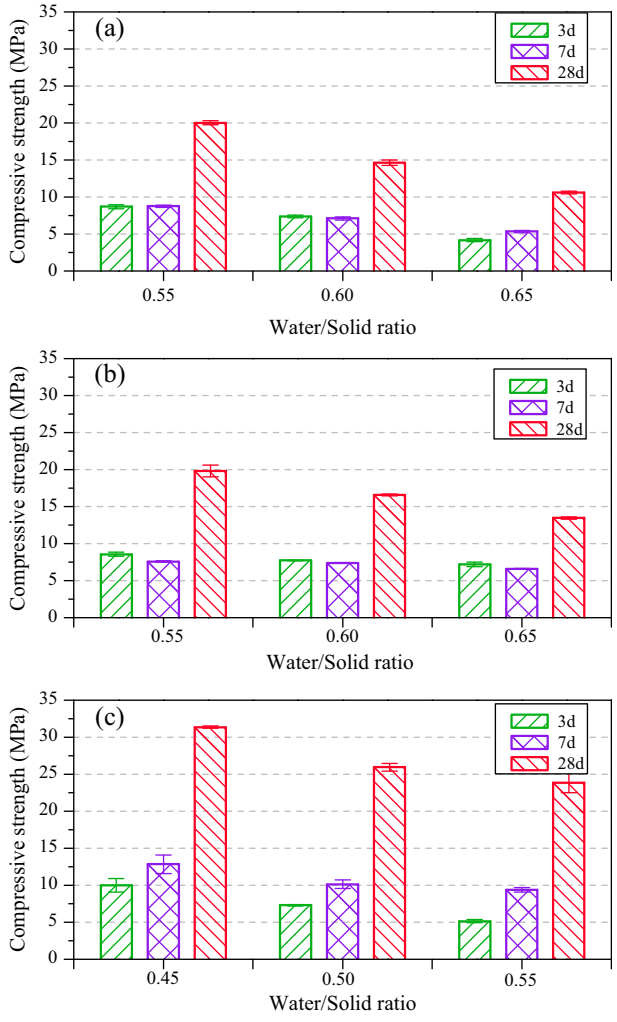

Fig. 4. The effect of water/solid ratio on the compressive strength of one-part geopolymer binders prepared from alkali–thermal activated RM: (a) G-10N-25S-A group; (b) G-15N-25S-A group; (c) G-10N-25S-B group with 0.5 wt% of sodium lignosulphonate as dispersant.

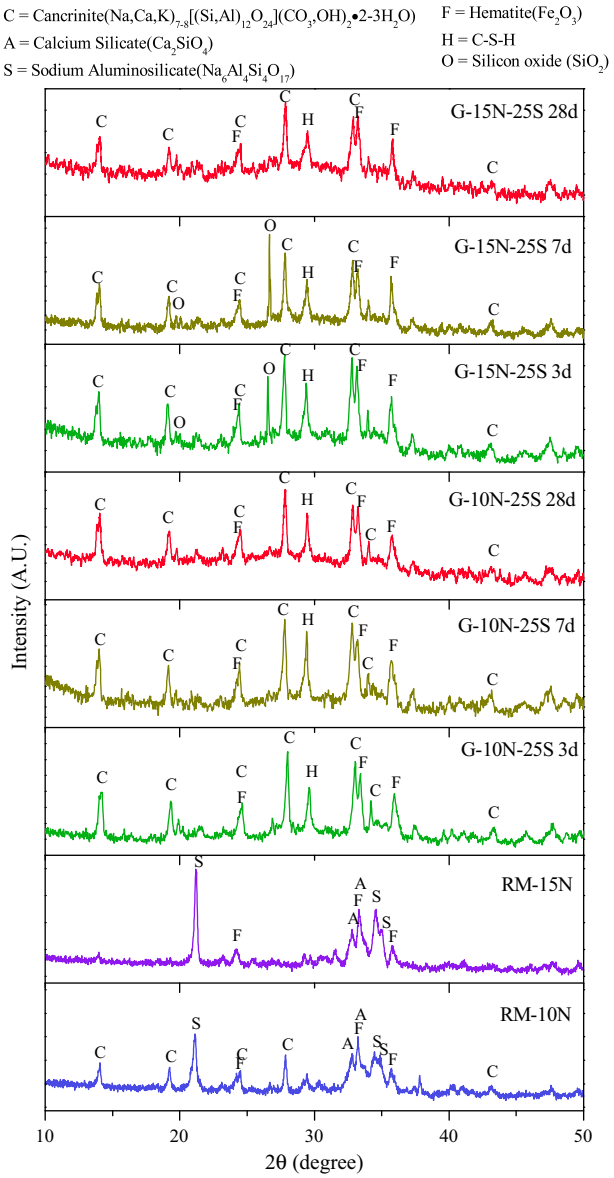

Fig. 5. The XRD patterns of alkali–thermal activated RM and one-part geopolymer binders cured for 3, 7, and 28 d with 25 wt% SF at the water/solid ratio of 0.65.

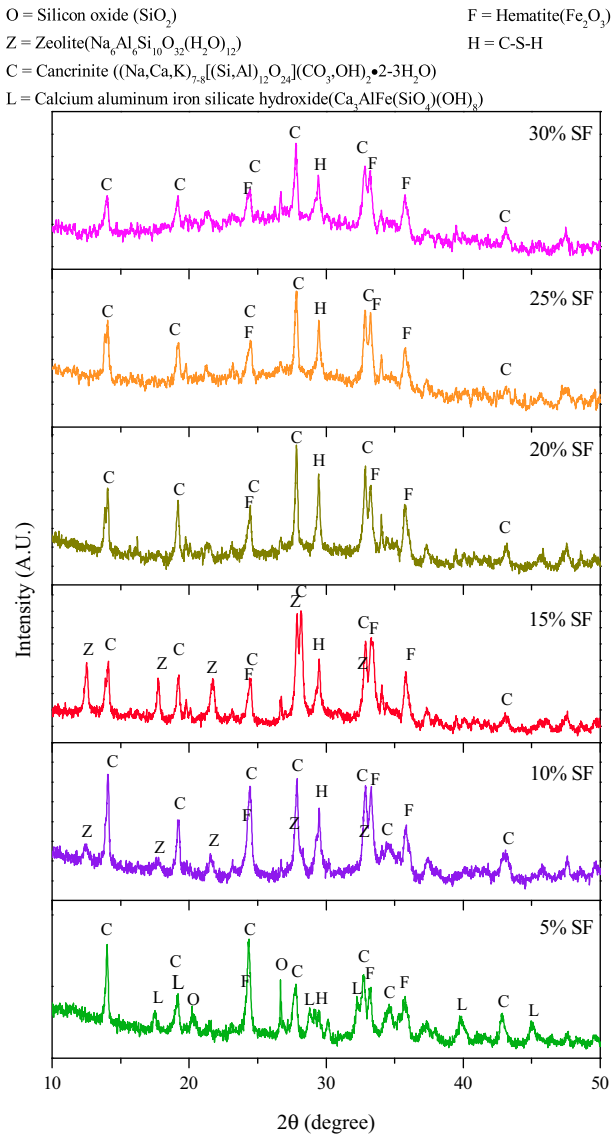

Fig. 6. The XRD patterns of one-part geopolymer binders prepared from RM-10N with 5, 10, 15, 20, 25, 30 wt% SF at the ratio of water/solid ratio of 0.65 cured for 28 d.

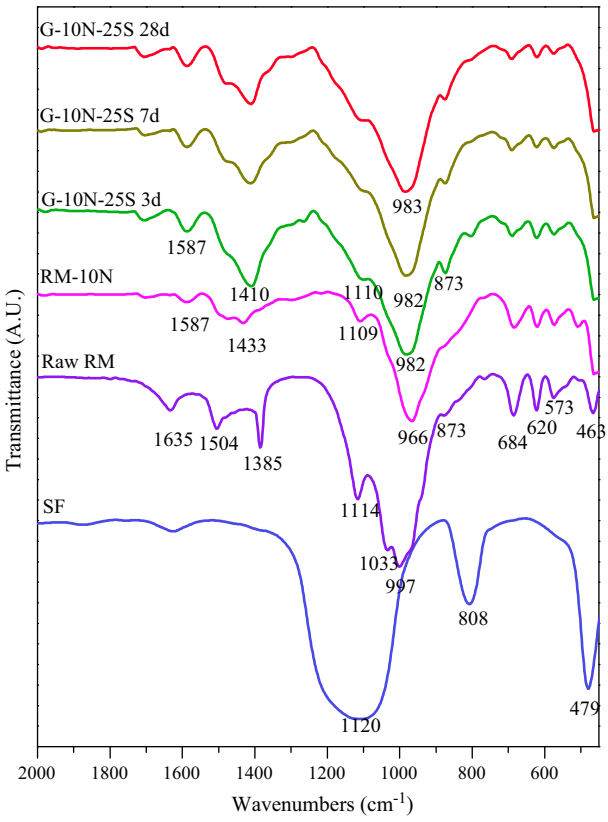

Fig. 7. FTIR spectra of SF, raw RM, RM-10N and G-10N-25S binders cured for 3 d, 7 d, 28 d.

3.4. Transformation of mineral phases in one-part geopolymer process

The XRD patterns of alkali–thermal activated RM samples (RM-10N and RM-15N) and the one-part geopolymer binders prepared from them with the addition of 25 wt% of SF (G-10N-25S and G-15N-25S) at various curing ages of 3 d, 7 d and 28 d are shown in Fig. 5. Most of the mineral phases in the raw RM such as gibbsite, calcite, muscovite, cancrinite, and katoite decompose after alkali–thermal activation, and the cancrinite in RM-15N sample decompose more thoroughly than that in RM-10N sample. Two new mineral phases, calcium silicate (Ca_2SiO_4) and sodium aluminosilicate ($Na_6Al_4Si_4O_{17}$), are formed in the alkali–thermal activated red mud, which could be the major phases contributing to the formation of alkaline environment and hardening of the geopolymer binder. The major characteristic peak of sodium aluminosilicate at 21.2° (2θ) in RM-15N is higher than that in RM-10N, implying that more sodium aluminosilicate in RM-15N is formed than that in RM-10N. All of the cancrinite in RM-15N have transformed into sodium aluminosilicate. This explains why the compressive strength of the binder made from RM-15N is higher than that from RM-10N at the water/solid ratio of 0.65.

In the geopolymer binders, both calcium silicate and sodium aluminosilicate hydrate and disappear, but a cancrinite group mineral is regenerated in the binders. CO_2 from the ambient atmosphere will react with the high alkaline pore solution in the binder to form carbonate. In the presence of CO_3^{2-} in the pore solution, aluminosilicates can transform to carbonate bearing cancrinite [30]. Calcium silicate hydrate appears in the binders due to the hydration of calcium silicate, and contributes to the strength of the binder. Some amorphous phases with a weak broad hump around 2θ of 25–35° are formed in the binders, which become more obvious with the curing age. The major feature of XRD patterns of typical geopolymers is a featureless "hump" centered at 2θ of 27–29° [11]. Thus it can be inferred that typical geopolymer products are formed in the binders. The difference between G-15N-25S and G-10N-25S is mainly the presence of a crystalline silicon oxide. A large number of crystalline silicon oxide with a characteristic peak at 2θ of 26.7° are identified in G-15N-25S samples cured for 3 and 7 d. The intensity of the characteristic peak of silicon oxide increases in the binder cured for 7 d and disappears in the binder cured for 28 d. The formation of silicon oxide phase is attributed to the reprecipitation of SiO_3^{28} formed by the dissolution of SF in the high alkaline liquid phase. Since the alkalinity of the liquid phase in G-15N-25S is stronger than that in G-10N-25S, SF dissolved more rapidly in G-15N-25S, and the dissolved silica would more likely to reprecipitate before polymerizing with dissolved sodium aluminosilicate in G-15N-25S.

Most of RM contain appreciable levels of Fe, mainly in the form of hematite. The effect of Fe on the geopolymerization was a focus of concern. Daux et al. [31] found that in the dissolution of basaltic glasses containing significant levels of network-forming Fe^{3+} in

slightly alkaline solutions, dissolved Fe reprecipitated much faster than Si and Al. Deventer et al. reported that any reactive Fe present during geopolymerization of fly ash reprecipitated very rapidly as hydroxide or oxy-hydroxide phases, removing OH^- ions from the solution phase and therefore slowing the dissolving of the remaining fly ash particles as well as providing nucleation sites [13]. The Fe in RM have undergone the reprecipitation process in the digestion of bauxite by caustic soda to produce alumina. Few of Fe in RM exist as network former or network modifier in glassy phases like fly ash. Fig. 5 shows that the hematite remained the same after alkali–thermal activation and geopolymerization, which implied that the Fe in RM had few influences on the geopolymerization.

The XRD patterns of the one-part geopolymer binders prepared from RM-10N with various additions of 5, 10, 15, 20, 25, 30 wt% of SF cured for 28 d are shown in Fig. 6. For the G-10N-5S binder with the addition of 5 wt% of SF, a particular phase, calcium aluminum iron silicate hydroxide ($Ca_3AlFe(SiO_4)(OH)_3$) is generated, which is a zeolitic mineral like cancrinite. It might be formed from cancrinite due to the replacement of Al by Fe of the same trivalent charge. In addition, crystalline silicon oxide is also identified. With the addition of 10 and 15 wt% of SF, a phase of zeolite with a SiO_2/Al_2O_3 molar ratio of 10/3 is formed, especially in the G-10N-15S binder. Geopolymer is a class of amorphous zeolite-like materials with similar chemical composition, but absence of the distinctive zeolitic structure [32]. The physicochemical conditions for synthesis of zeolites are quite similar to those for geopolymerization. But zeolites are commonly synthesized in hydrothermal conditions with higher temperatures over 80 °C and higher water content [33,34]. It's interesting to find a type of zeolite formed under ambient temperatures. Longer reaction times tend to give more crystalline products [33], which may explain the formation of zeolite at the curing age of 28 d. With the addition of more than 20 wt% of SF, the broad hump centered at 2θ of 27–29° in the binders appears obviously, implying the formation of more amorphous geopolymerization products. This is consistent with the formulation designs in Table 2 and the result of compressive strength in Fig. 3.

3.5. Transformation of FTIR spectra in one-part geopolymer process

The phase transformations are also identified by FTIR as shown in Fig. 7. The most significant transformation is that the bands attributed to asymmetric stretching vibrations of T–O (T = Al, Si) at 1033 cm^{-1} and 997 cm^{-1} in the raw RM shift to 963 cm^{-1}. In addition, the intensity of the bands attributed to asymmetric stretching of Si–O–Si bonds at 1114 cm^{-1} in the raw RM decreases after alkali–thermal activation. A narrow band associated with the T–O bonds is formed in RM-10N. It was reported that the band associated with T–O stretching vibrations shifted downward with rises in the content of tetrahedrally positioned Al atom in the system [35]. It could be inferred from the transformation of asymmetric stretching vibrations T–O that alkali–thermal activation promotes the substitution of Al^{3+} for Si^{4+}.

The intensity of the bands attributed to bending vibrations of Al–OH at 1385 cm^{-1}, stretching vibrations of O–C–O at 873 cm^{-1} and 1400–1500 cm^{-1}, and bending vibrations of H–O–H at 1500–

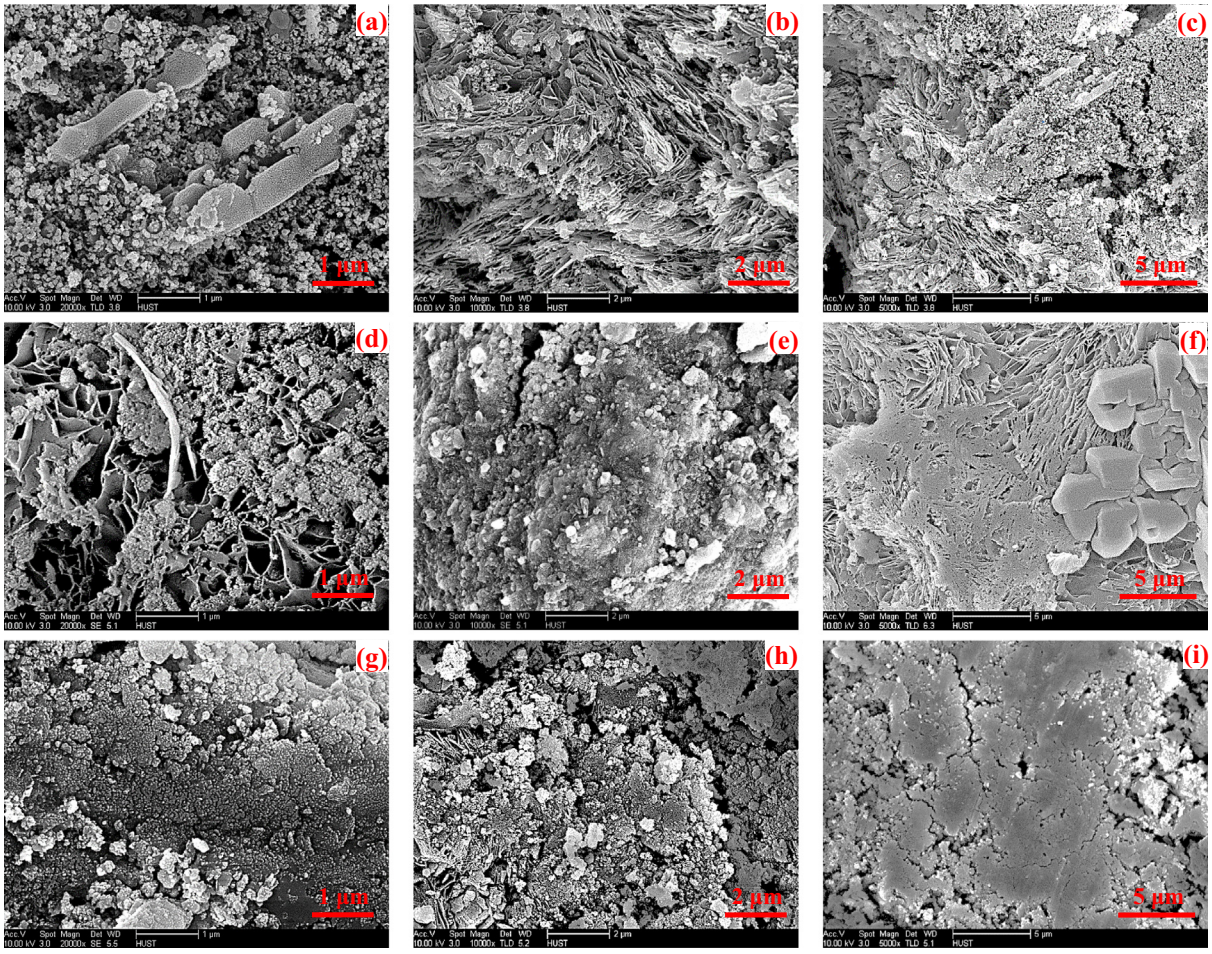

Fig. 8. SEM images of G-10N-25S binders cured for 3 d (a–c), 7 d (d–f), and 28 d (g–i).

1700 cm^{-1} in the raw RM decrease significantly in the RM-10N because of the decomposition of the minerals in raw RM. The absorption bands of O–C–O and H–O–H appear again in the geopolymer binders, implying the hydration and carbonation of the binders.

The FTIR spectrum of SF exhibited absorption bands attributed to the asymmetric stretching of Si–O–Si bonds at 1120 cm^{-1}, symmetric stretching of Si–O–Si bonds at 808 cm^{-1} [36] and bending vibrations of Si–O–Si and O–Si–O at 479 cm^{-1} [37]. These absorption bands are not significant in the geopolymer binders, implying the dissolution of SF. The dissolved silica from SF participates in the geopolymerization and improves the SiO_2/Al_2O_3 ratio of the aluminosilicate gel. Thus the T–O stretching vibrations band move to higher frequency of 982 cm^{-1} in the geopolymer binders. Compared with the reported fly ash based geopolymer [35,38], the bands generated by T–O bridge stretching vibrations of RM based geopolymer appear at a lower frequency than 999–1026 cm^{-1} of fly ash based geopolymer, which should be due to relatively lower Si/Al ratio in the structure. The FTIR spectra of the geopolymer binders cured for different ages show no significant differences. Little evolutions in function of curing age of this one-part geopolymer could be obtained from the FTIR data.

3.6. Morphological and elemental analysis of the binders

The morphological transformations of the core regions during the geopolymerization process of the one-part geopolymer binder G-10N-25S are shown in Fig. 8. Two separate phases are formed in the G-10N-25S binder cured for 3 d (Fig. 8(c)): large quantities of 50 nm size particulates (magnified in Fig. 8(a)) and stacked lamella (magnified in Fig. 8(b)). It is inferred that the particulate phase contains many undissolved SF particles, and the stacked lamella phase is the hydration product of the alkali–thermal activated RM. As the curing time extends to 7 d, the phase of undissolved SF particles disappears. The lamellar phase dissolves again and then polymerizes with the dissolved silica to form nanosized geopolymeric micelles [11], as shown in Fig. 8(d). Fig. 8(f) has shown the morphology transformation of stacked lamella to blocks, which should be a coexistence of geopolymer gel and calcium silicate hydrate. The SEM images of the binder cured for 28 d have shown the process of geopolymeric micelles aggregates to high dense matrices. Fig. 8(h) shows the intermediate state of geopolymeric micelles that aggregates to geopolymeric matrices. The final geopolymerization products have high dense matrices as shown in Fig. 8(i).

4. Conclusions

In this work, we have synthesized a novel one-part geopolymer cement by using Bayer red mud as the main raw material through alkali–thermal activation, with silica fume as an additive to improve the SiO_2/Al_2O_3 molar ratio. This approach can greatly contribute to the beneficial reuse of massive Bayer red mud.

The conclusions are as follows:

1. SF worked well in improving the long-term strength of the one-part geopolymer binder by improving the stability of the structure. At the addition of SF of 20–30 wt%, the designed one-part geopolymer approached the satisfactory formulations and presented higher compressive strength, especially at 25 wt%.
2. The compressive strengths of the binders cured for 28 d increase significantly when the water/solid ratio decreases. The water/solid ratio of geopolymer binder can be reduced to 0.45 by adding 0.5 wt% of sodium lignosulphonate as dispersant, and the compressive strength of the G-10N-25S binder cured for 28 d reached a maximum up to 31.5 MPa.
3. Soluble sodium aluminosilicate that formed in the alkali–thermal activated RM will dissolve in water and form an alkaline environment, which contributed to dissolving SF. The dissolved silica participated in the geopolymerization of Al–O and Si–O to form geopolymer micelles, thus improved the Si/Al ratio of geopolymerization, which will lead to a more stable structure. Geopolymer micelles aggragated to form amorphous geopolymer matrices in the binder completely cured.

Acknowledgments

The authors would like to appreciate the financial support of the New Century Excellent Talents Project of Ministry of Education (NCET-10-0392), the Public Welfare Program of Environmental Protection Ministry of China (201509056), and the Project of Innovative and Interdisciplinary Team of Huazhong University of Science and Technology (HUST) (0118261077). The authors would also like to appreciate the Analytical and Testing Center of HUST for the microstructure characterization tests.

References

[1] M. Gräfe, G. Power, C. Klauber, Bauxite residue issues: III. Alkalinity and associated chemistry, Hydrometallurgy 108 (2011) 60–79.
[2] A.R. Hind, S.K. Bhargava, S.C. Grocott, The surface chemistry of Bayer process solids: a review, Colloids Surf. A 146 (1999) 359–374.
[3] G. Power, M. Gräfe, C. Klauber, Bauxite residue issues: I. Current management, disposal and storage practices, Hydrometallurgy 108 (2011) 33–45.
[4] A. Gelencsér, N. Kováts, B. Turóczi, Á. Rostási, A. Hoffer, K. Imre, I. Nyirő-Kósa, D. Csákberényi-Malasics, Á. Tóth, A. Czitrovszky, A. Nagy, S. Nagy, A. Ács, A. Kovács, Á. Ferincz, Z. Hartyáni, M. Pósfai, The red mud accident in Ajka (Hungary): characterization and potential health effects of fugitive dust, Environ. Sci. Technol. 45 (2011) 1608–1615.
[5] Y. Liu, R. Naidu, Hidden values in bauxite residue (red mud): recovery of metals, Waste Manage. 34 (2014) 2662–2673.
[6] A. Bhat, H. Abdul Khalil, I.U.H. Bhat, A. Banthia, Development and characterization of novel modified red mud nanocomposites based on poly (hydroxy ether) of bisphenol A, J. Appl. Polym. Sci. 119 (2011) 515–522.
[7] S. Sushil, V.S. Batra, Catalytic applications of red mud, an aluminium industry waste: a review, Appl. Catal. B: Environ. 81 (2008) 64–77.
[8] A. Bhatnagar, V.J. Vilar, C.M. Botelho, R.A. Boaventura, A review of the use of red mud as adsorbent for the removal of toxic pollutants from water and wastewater, Environ. Technol. 32 (2011) 231–249.
[9] X.M. Liu, N. Zhang, Utilization of red mud in cement production: a review, Waste Manage. Res. 29 (2011) 1053–1063.
[10] C. Klauber, M. Gräfe, G. Power, Bauxite residue issues: II. Options for residue utilization, Hydrometallurgy 108 (2011) 11–32.
[11] J. Davidovits, Geopolymer Chemistry and Applications, 3rd ed., Geopolymer Institute, Saint-Quentin, 2011.
[12] J. Davidovits, Geopolymers – inorganic polymeric new materials, J. Therm. Anal. 37 (1991) 1633–1656.
[13] J.S.J. van Deventer, J.L. Provis, P. Duxson, G.C. Lukey, Reaction mechanisms in the geopolymeric conversion of inorganic waste to useful products, J. Hazard. Mater. 139 (2007) 506–513.
[14] D. Khale, R. Chaudhary, Mechanism of geopolymerization and factors influencing its development: a review, J. Mater. Sci. 42 (2007) 729–746.
[15] D.D. Dimas, I.P. Giannopoulou, D. Panias, Utilization of alumina red mud for synthesis of inorganic polymeric materials, Miner. Process. Extract. Metall. Rev. 30 (2009) 211–239.
[16] J. He, J. Zhang, Y. Yu, G. Zhang, The strength and microstructure of two geopolymers derived from metakaolin and red mud-fly ash admixture: a comparative study, Constr. Build. Mater. 30 (2012) 80–91.
[17] G. Zhang, J. He, R. Gambrell, Synthesis, characterization, and mechanical properties of red mud-based geopolymers, Transp. Res. Rec.: J. Transp. Res. Board 2167 (2010) 1–9.
[18] A. Kumar, S. Kumar, Development of paving blocks from synergistic use of red mud and fly ash using geopolymerization, Constr. Build. Mater. 38 (2013) 865–871.
[19] J. He, Y. Jie, J. Zhang, Y. Yu, G. Zhang, Synthesis and characterization of red mud and rice husk ash-based geopolymer composites, Cem. Concr. Comp. 37 (2013) 108–118.

[20] N. Ye, J. Yang, X. Ke, J. Zhu, Y. Li, C. Xiang, H. Wang, L. Li, B. Xiao, Synthesis and characterization of geopolymer from Bayer red mud with thermal pretreatment, J. Am. Ceram. Soc. 97 (2014) 1652–1660.
[21] D. Koloušek, J. Brus, M. Urbanova, J. Andertova, V. Hulinsky, J. Vorel, Preparation, structure and hydrothermal stability of alternative (sodium silicate-free) geopolymers, J. Mater. Sci. 42 (2007) 9267–9275.
[22] D. Feng, J.L. Provis, J.S. Deventer, Thermal activation of albite for the synthesis of one-part mix geopolymers, J. Am. Ceram. Soc. 95 (2012) 565–572.
[23] P. Duxson, J.L. Provis, Designing precursors for geopolymer cements, J. Am. Ceram. Soc. 91 (2008) 3864–3869.
[24] X. Ke, S.A. Bernal, N. Ye, J.L. Provis, J. Yang, One-part geopolymers based on thermally treated red mud/NaOH blends, J. Am. Ceram. Soc. 98 (2014) 5–11.
[25] W. Liu, J. Yang, B. Xiao, Review on treatment and utilization of bauxite residues in China, Int. J. Miner. Process. 93 (2009) 220–231.
[26] L.P. Ogorodova, L.V. Mel'chakova, M.F. Vigasina, L.V. Olysich, I.V. Pekov, Cancrinite and cancrisilite in the Khibina–Lovozero alkaline complex: thermochemical and thermal data, Geochem. Int. 47 (2009) 260–267.
[27] J. Plank, Applications of biopolymers and other biotechnological products in building materials, Appl. Microbiol. Biotechnol. 66 (2004) 1–9.
[28] E. Najafi Kani, A. Allahverdi, J.L. Provis, Efflorescence control in geopolymer binders based on natural pozzolan, Cem. Concr. Comp. 2011 (34) (2012) 25–33.
[29] C. Ruiz-Santaquiteria, J. Skibsted, A. Fernández-Jiménez, A. Palomo, Alkaline solution/binder ratio as a determining factor in the alkaline activation of aluminosilicates, Cem. Concr. Res. 42 (2012) 1242–1251.
[30] Y. Deng, J.B. Harsh, M. Flury, J.S. Young, J.S. Boyle, Mineral formation during simulated leaks of Hanford waste tanks, Appl. Geochem. 21 (2006) 1392–1409.
[31] V. Daux, C. Guy, T. Advocat, J.-L. Crovisier, P. Stille, Kinetic aspects of basaltic glass dissolution at 90 °C: role of aqueous silicon and aluminium, Chem. Geol. 142 (1997) 109–126.
[32] J.G.S. Van Jaarsveld, J.S.J. Van Deventer, L. Lorenzen, The potential use of geopolymeric materials to immobilise toxic metals: Part I. Theory and applications, Miner. Eng. 10 (1997) 659–669.
[33] J.L. Provis, G.C. Lukey, J.S.J. van Deventer, Do geopolymers actually contain nanocrystalline zeolites? A reexamination of existing results, Chem. Mater. 17 (2005) 3075–3085.
[34] R.I. Walton, F. Millange, D. O'Hare, A.T. Davies, G. Sankar, C.R.A. Catlow, An in situ energy-dispersive X-ray diffraction study of the hydrothermal crystallization of zeolite A. 1. Influence of reaction conditions and transformation into sodalite, J. Phys. Chem. B 105 (2000) 83–90.
[35] A. Fernández-Jiménez, A. Palomo, Mid-infrared spectroscopic studies of alkali-activated fly ash structure, Microporous Mesoporous Mater. 86 (2005) 207–214.
[36] S.A. Bernal, E.D. Rodríguez, R.M. de Gutiérrez, J.L. Provis, S. Delvasto, Activation of metakaolin/slag blends using alkaline solutions based on chemically modified silica fume and rice husk ash, Waste Biomass Valorization 3 (2012) 99–108.
[37] W. Lee, J. Van Deventer, Use of infrared spectroscopy to study geopolymerization of heterogeneous amorphous aluminosilicates, Langmuir 19 (2003) 8726–8734.
[38] M. Criado, A. Fernández-Jiménez, A. Palomo, Alkali activation of fly ash: Effect of the SiO_2/Na_2O ratio: Part I: FTIR study, Microporous Mesoporous Mater. 106 (2007) 180–191.